International Symposium
On Turbulence and Shear Flow
Phenomena (TSFP-8)
August 28 - 30, 2013 Poitiers, France

NUMERICAL AND MODELING STRATEGIES FOR THE SIMULATION OF THE CAMBRIDGE STRATIFIED FLAME SERIES

Renaud Mercier, Benoît Fiorina
Ecole Centrale Paris
CNRS, UPR 288, Laboratoire EM2C
Grande Voie des Vignes
92290 Châtenay-Malabry, France
renaud.mercier@ecp.fr

Fabian Proch, Andreas M. Kempf
Institute for Combustion and Gasdynamics (IVG)
Chair for Fluid Dynamics
University of Duisburg-Essen
Duisburg, 47048, Germany

ABSTRACT

The Cambridge stratified swirl burner (SwB) has been experimentally investigated for premixed and stratified flame regimes with non-swirling and swirling injection streams. The choice of an appropriate numerical and modeling strategy to capture both stabilization mechanism and turbulent flame propagation is a challenging issue. The present paper presents a comparison between two different approaches. The first one uses a Flame Surface Density (FSD) approach associated to a structured low-Mach code. The second one uses the Filtered Tabulated Chemistry for Large Eddy Simulation (F-TACLES) model implemented in an unstructured low-Mach code. LES results of the non reactive, fully premixed and stratified non-swirling cases are presented and discussed. A good agreement on velocity, mixing and temperature statistics is found for both approaches.

INTRODUCTION

To manage the flame temperature and therefore the pollutant formation, novel combustors are generally designed to operate in a premixed-like regime. As fuel and oxidizer are injected separately, a very fast mixing of both streams is needed prior to combustion. Even if the mixing is usually enhanced through high shear flows, it is however never perfect and the flame evolves in a "stratified" mixture that exhibits local fluctuations of equivalence ratio. The stabilization of these turbulent stratified flames, governed by aerodynamic, mixing and chemical effects, is then extremely complex.

To study the crossed effects of stratification intensity and turbulence level on the stabilization and propagation mechanism of stratified combustion, a co-annular methane-air burner introduced by Sweeney *et al.* (2011) has been recently investigated at Cambridge University and Sandia National Laboratories. The stratified swirl burner (SwB) is composed of two concentric tubes and a central bluff-body. Mass flow rate and fresh gas equivalence ratio are controlled independently in each tube while the outer stream can be either swirling or non-swirling. The flame is isolated from ambient perturbations by a surrounding air co-flow.

An experimental characterization of the thermochemical turbulent flame structure in both premixed and stratified cases has been proposed for non-swirling (Sweeney *et al.*, 2012*a*) and swirling (Sweeney *et al.*, 2012*b*, 2013) situations. An important result is that both premixed and stratified chemical flame structures in temperature space are found to be very close of unstrained premixed laminar flames. Nevertheless significant discrepancies on CO and H_2 species mass fractions for high temperatures are attributed to local stratification effects. Sweeney *et al.* (2011) also showed that the flame surface density was not dependent on the stratification level suggesting that the interaction between turbulent flow and the thin flame front was not impacted by local equivalence ratio heterogeneities.

Because of the reactive flow complexity the Large Eddy Simulation (LES) of the SwB flame series is challenging. Both the flow dynamics and the flame propagation in a stratified environment need to be captured and the choice of an appropriate combustion modeling strategy remains an open question. Considering the experimental results on both geometrical properties (Sweeney *et al.*, 2011) and chemical structure (Sweeney *et al.*, 2012*a*,*b*) of the SwB turbulent flames, it is consistent to assume that the turbulent flame front is only wrinkled by the turbulence while the inner flame structure is not affected and remains similar to an unstrained laminar flame. In this context, geometrical approaches can be used to model the flame-turbulence interaction as discussed in Veynante & Vervisch (2002).

The objective of this paper is to test the ability of two different geometrical approaches to capture both the stabilization mechanism and the turbulent propagation of the SwB non-swirling flame series. Both the Flame Surface Density (FSD) model introduced by Boger *et al.* (1998) and the Filtered Tabulated Chemistry for LES (F-TACLES) initially proposed by Fiorina *et al.* (2010) are considered. The two strategies mainly differ by the description of the chemical flame structure: the F-TACLES model uses chemistry tabulation while FSD formalism only conserves integrated variables as flame consumption speed. The paper is structured as follows. Both numerical and modeling strategies are described in the first section. Simulations of a non-reactive case, a reacting premixed case and a reacting stratified case are then presented and analysed.

NUMERICAL AND MODELING STRATEGIES

FSD and F-TACLES approaches are respectively implemented in a structured and an unstructured low-Mach codes. Numerical and modeling strategies are briefly detailed in this section.

Flame surface density approach

In this approach, the Favre-filtered governing equations for incompressible fluid flow of temperature dependent density are solved. Two additional transport equations are introduced to describe stratified combustion process. The mixture fraction z is a conserved scalar equal to 0 and 1 in pure air and fuel streams respectively. The filtered mixture fraction $\widetilde{z}$ transport equation, closed using a classical gradient assumption, reads:

$$\frac{\partial(\overline{\rho}\widetilde{z})}{\partial t}+\nabla\cdot(\overline{\rho}\widetilde{\mathbf{u}}\widetilde{z})=\nabla\cdot\left[\left(\frac{\mu}{S_c}+\frac{\mu_t}{S_{ct}}\right)\nabla\widetilde{z}\right] \quad (1)$$

where ρ, $\mathbf{u}$ and μ_t denote respectively density, flow velocity vector and turbulent viscosity while S_c and S_{ct} are respectively the laminar and turbulent Schmidt numbers taken equal to 0.7.

The progress variable c is defined from fuel species mass fraction as $c=(Y_F-Y_F^u(z))/(Y_F^b(z)-Y_F^u(z))$ where superscripts u and b denote unburnt and burnt states respectively. The transport equation of the filtered progress variable $\widetilde{c}$ is built here from the $Y_F=Y_{CH_4}$ species mass fraction balance equation as discussed in Domingo *et al.* (2002); Bray *et al.* (2005); Duwig & Fureby (2007) and reads:

$$\begin{aligned}\frac{\partial(\overline{\rho}\widetilde{c})}{\partial t}&+\nabla\cdot(\overline{\rho}\widetilde{\mathbf{u}}\widetilde{c})+\nabla\cdot[\overline{\rho}\,(\widetilde{\mathbf{u}c}-\widetilde{\mathbf{u}}\widetilde{c})]\\&=\overline{\nabla\cdot(\rho D\nabla c)}+\overline{\dot{\omega}_c}+\frac{2}{\widetilde{z}}\overline{\rho}D\nabla\widetilde{c}\cdot\nabla\widetilde{z}\end{aligned} \quad (2)$$

The filtered molecular diffusion term and reaction rate are modeled using the flame surface density approach initially proposed by Boger *et al.* (1998):

$$\overline{\nabla\cdot(\rho D\nabla c)}+\overline{\dot{\omega}_c}=\overline{(\rho S_d)}_s\Sigma_{gen} \quad (3)$$

where $\overline{(\rho S_d)}_s$ is the density weighted surface-averaged displacement speed. Neglecting curvature effects, $\overline{(\rho S_d)}_s$ can be recast as $\overline{(\rho S_d)}_s=\rho_0 S_l^0$ where S_l^0 denotes the unstretched laminar flame speed and ρ_0 the fresh gas density. The mixture fraction subgrid scale heterogeneities are accounted for using a top-hat FDF as proposed by Floyd *et al.* (2009). S_l^0 is determined as a function of fresh gas mixture fraction z computing 1-D freely-propagating premixed flames using detailed chemistry and varying fresh gas equivalence ratio. For that purpose, the Lindstedt (1997) detailed chemical scheme composed of 29 species and 141 reactions has been used. The flame surface density Σ_{gen} represents the unresolved wrinkling of the flame surface and is related to the subgrid scale wrinkling function Ξ as $\Sigma_{gen}=\Xi|\nabla\bar{c}|$. Ξ is estimated using the model proposed by Fureby (2005). Following the recommendations of Ma *et al.* (2013), the original model was slightly modified to achieve the correct limiting behaviour for a laminar flame. Therefore, both unresolved laminar and turbulent fluxes were taken into account:

$$\nabla\cdot[\overline{\rho}\,(\widetilde{\mathbf{u}c}-\widetilde{\mathbf{u}}\widetilde{c})]=-\frac{\mu_t}{S_{ct}}\nabla\tilde{c}+\rho_0 S_l^0\,(\tilde{c}-\tilde{c})\,\frac{\nabla\tilde{c}}{|\nabla\tilde{c}|} \quad (4)$$

The proposed FSD model has been implemented in the in-house LES low-Mach number code *PsiPhi* (Franchetti *et al.*, 2013; Marincola *et al.*, 2013). Favre-filtered low-Mach governing equations are solved using a 3D finite-volume formalism. The *PsiPhi* code handles structured cartesian grid of equidistant cubic cells. The convective term is discretised using a second-order central differencing scheme for momentum and a TVD limiter for scalars while a low storage third order Runge-Kutta scheme is used to perform time-advancement. Mass conservation is enforced by a predictor / corrector scheme combined with a projection method. Neumann conditions are applied at the outflow boundaries of the computational domain and pseudo-turbulent inflow conditions are created following the methodology proposed in Klein *et al.* (2003); Kempf *et al.* (2005).

Filtered Tabulated Chemistry for LES

The F-TACLES model has been developed to include complex chemistry effects in the LES formalism through chemistry tabulation. A set of 1-D freely propagating premixed flames is first computed with detailed chemistry varying fresh gas equivalence ratio within the flammability limits. As for the FSD approach, the Lindstedt (1997) chemical scheme is used in this work. The chemical subspace covered by the 1-D flames is mapped as a function of two coordinates following the FPI formalism introduced by Gicquel *et al.* (2000). The non-normalized progress variable Y_c is first defined from a linear combination of species mass fractions Y_k as $Y_c=\sum_{k=1}^{N_{sp}} n_k Y_k$ where n_k is the weighting coefficient associated to the kth species. In this work, Y_c is chosen as $Y_c=Y_{CO}+Y_{CO_2}$. The second coordinate is the mixture fraction z used to identify fresh gas equivalence ratio ϕ. As for the FSD approach, z evolves between 0 in pure air and 1 in fuel stream.

The FPI chemistry tabulation method is then coupled with the LES equations following the F-TACLES formalism. Both filtered non-normalized progress variable $\widetilde{Y_c}$ and filtered mixture fraction $\widetilde{z}$ are resolved during the LES computation. As for the FSD model, $\widetilde{z}$ follows the filtered balance equation given in Eq. 1 while $\widetilde{Y_c}$ equation reads:

$$\begin{aligned}\frac{\partial\bar{\rho}\widetilde{Y_c}}{\partial t}&+\nabla\cdot(\bar{\rho}\widetilde{\mathbf{u}}\widetilde{Y_c})=\nabla\cdot\left(\overline{\sum_{k=1}^{N_{sp}}[n_k\rho Y_k V_k]}\right)\\&-\nabla\cdot\left(\bar{\rho}\widetilde{\mathbf{u}Y_c}-\bar{\rho}\widetilde{\mathbf{u}}\widetilde{Y_c}\right)+\bar{\rho}\widetilde{\dot{\omega}}_{Y_c}\end{aligned} \quad (5)$$

Fiorina *et al.* (2010) proposed to close the three RHS terms by explicitly filtering the 1-D laminar premixed flames introduced in the previous section. This methodology has been extended to stratified flames by Auzillon *et al.* (2012). The filtered progress variable reaction rate then reads:

$$\bar{\rho}\widetilde{\dot{\omega}}_{Y_c}=\Xi\int_0^1\langle\rho\dot{\omega}_{Y_c}|z=z'\rangle P(z')dz', \quad (6)$$

where $P(z')$, the Filtered Density Function (FDF) of the mixture fraction, accounts for subgrid scale mixture fraction heterogeneities. In practice, the mixture fraction FDF is approximated with a β distribution parametrized by $\widetilde{z}$ and $\widetilde{z''^2}$. The flame surface wrinkling factor Ξ is modeled following the Charlette *et al.* (2002) formulation recently corrected by Wang *et al.* (2011) while the conditional filtered value of the reaction rate $\langle \rho \dot{\omega}_{Y_c} | z = z' \rangle$ is estimated as:

$$\langle \rho \dot{\omega}_{Y_c} | z = z' \rangle = \int_{-\infty}^{+\infty} \rho^* \dot{\omega}^*_{Y_c}(x'_n, z') G_\Delta(x^*_n - x'_n) dx'_n \quad (7)$$

where the superscript * denotes quantities extracted from constant equivalence ratio 1-D flames. x^*_n is the spatial coordinate along the normal direction to the flame front and G_Δ a Gaussian filter of size Δ. In practice, Δ is chosen to ensure that the filtered flame front is well resolved on the LES grid.

The filtered molecular diffusion term is closed introducing the α_{Y_c} correction factor as $\sum_{k=1}^{N_{sp}} [n_k \rho Y_k V_k] = \alpha_{Y_c}[\widetilde{Y}_c, \widetilde{z}, \widetilde{z''^2}, \Delta] \rho_0 D_0 \nabla \widetilde{Y}_c$ where ρ_0 and D_0 are reference values for the density and the molecular diffusion coefficient, respectively, corresponding here to unburnt gas values. The correction factor α_{Y_c} is tabulated from 1-D filtered premixed flames as:

$$\alpha_{Y_c}[\widetilde{Y}_c, \widetilde{z}, \widetilde{z''^2}, \Delta] = -\frac{\overline{\sum_{k=1}^{N_{sp}} \left(n_k \rho^* Y^*_k V^*_k\right)}}{\left(\rho_0 D_0 \frac{\partial \widetilde{Y^*_c}}{\partial x^*_n}\right)} \quad (8)$$

The unresolved transport term is closed following a similar procedure:

$$\nabla \cdot \left(\bar{\rho}\widetilde{\mathbf{u}Y_c} - \bar{\rho}\widetilde{\mathbf{u}}\widetilde{Y_c}\right) = \Xi \Omega_{Y_c}[\widetilde{Y}_c, \widetilde{z}, \widetilde{z''^2}, \Delta] + \nabla \cdot \left((\Xi - 1)\alpha_{Y_c} \rho_0 D_0 \nabla \widetilde{Y}_c\right) \quad (9)$$

where the first RHS term is estimated from 1-D filtered premixed flames as $\Omega_{Y_c}[\widetilde{Y}_c, \widetilde{z}, \widetilde{z''^2}, \Delta] = \overline{\rho^*_0(z) S^*_l(z) \frac{\partial Y^*_c}{\partial x^*_n}} - \overline{\rho^*_0(z) S^*_l(z)} \frac{\partial \widetilde{Y^*_c}}{\partial x^*_n}$.

$\widetilde{\dot{\omega}}_{Y_c}$, α_{Y_c} and Ω_{Y_c} are stored in a 4-D look-up database and accessed during the LES computation where $\widetilde{Y}_c$, $\widetilde{z}$ and $\widetilde{z''^2}$ are transported. Further details on the generation of the filtered thermochemical database can be found in Fiorina *et al.* (2010) and Auzillon *et al.* (2012).

The F-TACLES model has been implemented in the YALES2 LES low-Mach number code described by Moureau *et al.* (2011). YALES2 is based on a finite volume formulation and handles unstructured meshes. A centered fourth-order scheme is used for spatial discretization while a fourth-order temporal scheme is used to perform time integration of convective terms. As for the *PsiPhi* code, a predictor / corrector scheme is used to solve the momentum balance equation. Turbulent inlet boundary conditions are performed by adding Homogeneous and Isotropic Turbulence (HIT) to the imposed velocity profiles.

Consistency of the modeling approaches

To ensure a relevant comparison between the numerical results of both strategies, it is important to note that all the 1-D premixed flame computations used for F-TACLES and FSD are achieved using the same detailed chemical scheme (Lindstedt, 1997). On the one hand, the closure methodology proposed in the F-TACLES model is based on the tabulation of the thermochemical flame structure. On the other hand, the FSD approach uses variables integrated across the flame front as the laminar flame consumption speed S^0_l. Finally, both FSD and F-TACLES models assume that the propagation speed S_Δ of the filtered flame front expresses $S_\Delta = \Xi \widetilde{S}_l$ where Ξ is the subgrid scale flame wrinkling. $\widetilde{S}_l$ reads:

$$\widetilde{S}_l = \frac{1}{\overline{\rho}_0} \int_0^1 \rho_0(z') S_l(z') P(z') dz' \quad (10)$$

where $\rho_0(z)$, the fresh gas density, is a function of the mixture fraction z.

INVESTIGATED CONFIGURATIONS

The Cambridge stratified swirl burner (SwB) consist in two concentric tubes surrounding a central bluff-body (Sweeney *et al.*, 2011). A longitudinal cut of the SwB burner is shown in Fig. 1.

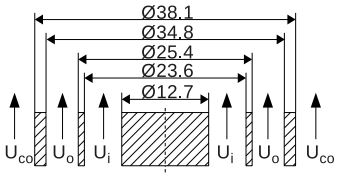

Figure 1. Cross section of the axisymmetric SwB burner

The two injected methane-air streams are controlled separately in terms of mass flow rate and fresh gas equivalence ratio. The inner stream (i) is non-swirling while the outer stream (o) can be either swirling or non-swirling. Only non-swirling cases have been considered in this work. A 0.4 m.s^{-1} air co-flow (co) isolates the flame from ambient perturbations. The three different inlet configurations presented in Tab. 1 are studied in this paper. The non-reacting case (SwBc) is first computed to validate the two numerical approaches. Then the fully premixed case (SwB1) is considered to compare modeling strategies when subgrid scale mixture fraction heterogeneities do not impact the flame propagation. Finally, the stratified case (SwB5) is computed to compare FSD and F-TACLES models when equivalence ratio heterogeneities affect the flame front.

NON REACTIVE FLOW SIMULATIONS

The LES of the non reactive case (SwBc) is performed with both the *PsiPhi* and YALES2 codes on a coarse and a finer mesh to verify mesh convergence. The σ-model recently proposed by Nicoud *et al.* (2011) is used for modelling of the subgrid scale (SGS) stress tensor in both codes,

Table 1. Boundary conditions.

Case	$\phi_i[-]$	$\phi_o[-]$	$\overline{U_i}[\frac{m}{s}]$	$\overline{U_o}[\frac{m}{s}]$	$\overline{U_{co}}[\frac{m}{s}]$
SwBc	-	-	8.31	18.7	0.4
SwB1	0.75	0.75	8.31	18.7	0.4
SwB5	1.0	0.5	8.31	18.7	0.4

Table 2. Summary of the mesh grids used in the present study. The "SwB" column lists the simulations performed using the associated mesh. Δ_x represents the characteristic mesh size in the combustion zone while N_{nd} is the total number of nodes. L_t holds for the injection tubes length included into the computational domain.

Mesh	SwB	Code	Type	Δ_x [mm]	L_t [mm]	N_{nd}
P1	c, 1, 5	*PsiPhi*	Struct.	0.5	20	13.10^6
P2	c	*PsiPhi*	Struct.	0.25	20	105.10^6
Y1	c,1,5	YALES2	Unstruct.	0.5	100	6.10^6
Y2	c	YALES2	Unstruct.	0.25	100	17.10^6

the modelling constant is set to $C_\sigma = 1.5$. The investigated meshes are summarized in Tab. 2.

Mean and RMS of the velocity field are compared to Laser Doppler Anemometry (LDA) experimental data (Zhou *et al.*, 2013) of SwBc case for four different distances from the burner exit (Z = 2, 10, 30 and 50 mm). Axial velocity statistics for the four computations detailed in Tab. 2 are presented in Fig. 2. This figure shows a very good agreement of both mean and RMS axial velocity profiles between the four LES and the experiments.

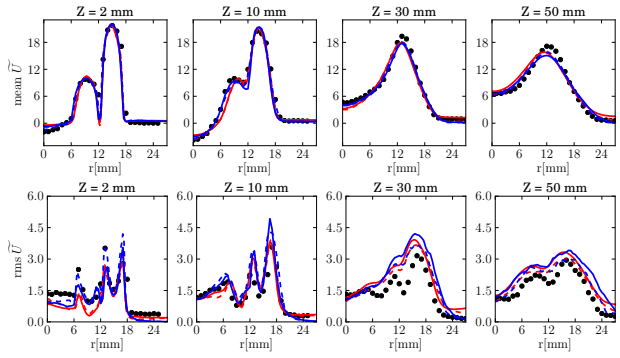

Figure 2. Mean (top) and RMS (bottom) axial velocity $\widetilde{U_z}$ profiles for non reactive (SwBc) case. Legend : — *PsiPhi* - P1 (coarse) mesh. - - - *PsiPhi* - P2 (fine) mesh. — YALES2 - Y1 (coarse) mesh. - - - YALES2 - Y2 (fine) mesh. • • Experiments (LDA).

Figure 2 also shows that both P1 and Y1 coarse meshes are sufficient to capture mean velocity fields. Finer meshes only increase the amount of resolved kinetic energy improving the overall resolved fluctuations levels. It is also worth noting that both the *PsiPhi* and YALES2 codes are predicting similar mean and RMS velocity fields.

FULLY PREMIXED FLAME SIMULATIONS

This section is devoted to the simulation of the fully premixed flame SwB1. Only coarse meshes P1 and Y1 are used here since they both provide a good description of the aerodynamics and mixing in the SwBc case. The F-TACLES filter size is $\Delta = 2.5$mm and can be compared to the thermal flame thickness δ_l^0 through the ratio $\Delta/\delta_l^0 = 5$. Both FSD and F-TACLES mixture fraction FDF have been forced to a δ distribution.

The SwB1 flame is stabilized by the burnt gases recirculation zone (RZ) induced by the central bluff-body. In the vicinity of the RZ (0mm<Z<20mm), the flame base is weakly turbulent while the flame surface is strongly disturbed by turbulence futher downstream (Z>20mm). Figure 3 plots mean and RMS temperature profiles for the SwB1 case. The mean flame brush position is fairly predicted by both simulations. Measured temperature fluctuations show that flame front fluctuations are lower near the burner exit whereas RMS peaks increase and become broader when the flame front crosses the shear layer induced between streams 1 and 2. This behavior is well predicted by both simulations. RMS temperature profiles far for the burner exit (Z>30mm) are however broader than the measured ones.

Figure 4 plots the local equivalence ratio Φ computed from to the resolved filtered mixture fraction $\widetilde{z}$ for Y1 and P1 simulations of the SwB1 case. Numerical results are compared with experimental measurements provided in Sweeney *et al.* (2012*a*,*b*). The broadening of the mean flame brush, over-predicted by both simulations, may be due to the slight misprediction of the mean equivalence ratio profiles far from the burner exit (Z>30mm). An important elevation of equivalence ratio levels within the bluff-body RZ (Z<30mm) is noted. This phenomenon has been experimentally investigated by Barlow *et al.* (2012); Dunn & Barlow (2013) and seems to result from preferential diffusion of H_2 and H_2O toward the reactants followed by convective transport of these species away from the local flame brush. This explanation has been recently confirmed by numerical simulations conducted by Katta & Roquemore (2013) and Nambully (2013). It is worth noting that this particular phenomenon is located near the burner exit where the flame base interacts with the bluff-body RZ. However, this complex transport of the chemical species out of the flame front, not accounted for by both FSD and F-TACLES models, does not impact the mean flame brush prediction.

STRATIFIED FLAME SIMULATIONS

The Large Eddy Simulation of the stratified case SwB5 is now presented. Both aerodynamics and stabilization process are very similar to the fully premixed case. Only the inner and outer stream equivalence ratii are modified (See Tab.1). Both FSD and F-TACLES computations have been performed on the same meshes as for the SwB1 case (P1 and Y1 respectively). Mixture fraction FDF are used here to account for the effects of the equivalence ratio stratification induced by the shear/mixing layer between streams 1 and 2.

Figure 5 displays an isosurface of filtered progress variable reaction rate $\bar{\rho}\widetilde{\dot{\omega}}_{Y_c}$ colored by fresh gas equivalence ratio. The flame is divided in two parts, namely part I and part II in Fig. 5. In part I, the flame front behaves like a fully premixed jet flame. Very few resolved flame wrinkling patterns are noted, suggesting that the flame stabilized by the bluff-body RZ, is weakly turbulent. In part II, the mix-

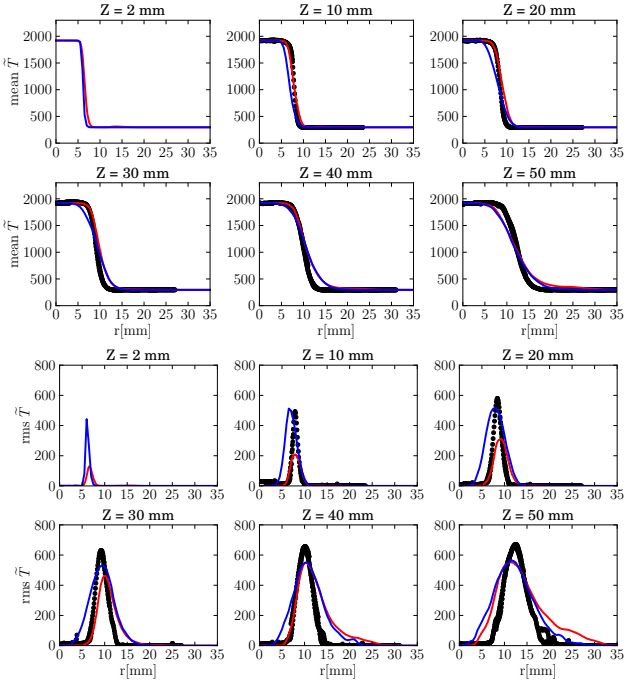

Figure 3. Mean (top) and RMS (bottom) temperature $\widetilde{T}$ profiles for the fully premixed (SwB1) case. Legend : — FSD model - P1 mesh. — F-TACLES model - Y1 mesh. • • Experiments.

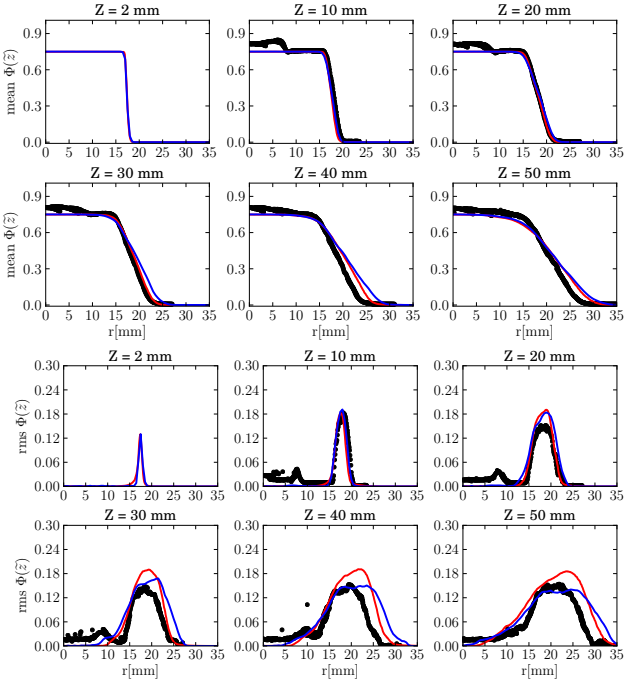

Figure 4. Mean (top) and RMS (bottom) equivalence ratio $\Phi(\widetilde{z})$ profiles for the fully premixed (SwB1) case. Legend : — FSD model - P1 mesh. — F-TACLES model - Y1 mesh. • • Experiments.

ture fraction stratification interacts further downstream with the highly wrinkled resolved flame front. Mean and RMS temperature profiles are compared to experimental data in Fig. 6. The mean flame brush is properly predicted and resolved. The RMS temperature levels is higher than in the SwB1 case. This is attributed to the higher equivalence ratio ($\Phi_i = 1.0$) at the flame base in the SwB5 case leading to an increase in mean flame angle compared to the SwB1 case ($\Phi_i = 0.75$). The flame interaction with the shear layer between streams 1 and 2 is then enhanced.

Comparisons of measured and simulated equivalence ratio profiles for the SwB5 case are shown in Fig. 7. This plot shows that near-burner preferential diffusion effects are also found in the SwB5 case.

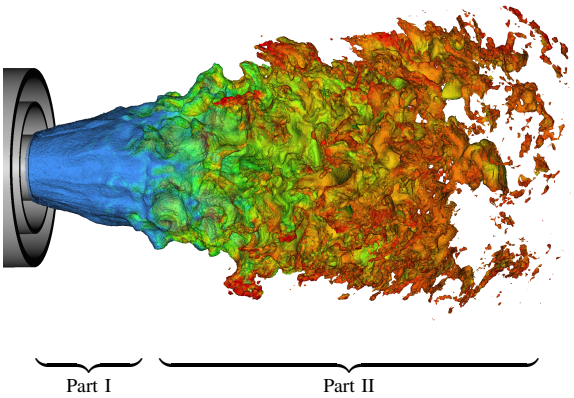

Figure 5. Isosurface of filtered progress variable reaction rate $\bar{\rho}\widetilde{\dot{\omega}}_{Y_c}$ colored by fresh gas equivalence ratio Φ for the stratified (SwB5) case.
Legend : ■ $\Phi = 1.0$. ■ $\Phi = 0.5$.

CONCLUSIONS

This contribution aimed to present the Large Eddy Simulation of the non reactive (SwBc), premixed (SwB1) and stratified (SwB5) cases. Both FSD and F-TACLES models have been selected for this study. LES results have been compared to the experimental data. Focus has been made on mean and RMS velocity, mixing and temperature predictions by the LES computations. Theses variables are compulsory to ensure a correct capture of the turbulent flame position and dynamics. They are reasonably well captured by both the FSD and F-TACLES approaches. An important conclusion is that the preferential diffusion phenomenon, not considered in the selected models, does not seem to control the mean flame position in both premixed and stratified cases. Further comparisons and analysis are in progress in particular on the impact of both mixture fraction FDF and subgrid scale wrinkling modeling assumptions.

ACKNOWLEDGEMENTS

The authors thank Dr. Mark Sweeney and Prof. Simone Hochgreb for providing experimental data. Dr. Vincent Moureau is gratefully acknowledged for his help.

This work was supported by the ANR-10-EESI-05 Grant of the French Ministry of Research. This work was performed using HPC resources from GENCI-CINES and GENCI-IDRIS (Grant 2011-x2011020164).

The authors also gratefully acknowledge funding provided from the state of Nordrhein-Westfalen, Germany. Research has been supported by the Center for Computational Sciences and Simulation (CCSS) of the University of Duisburg-Essen, Germany.

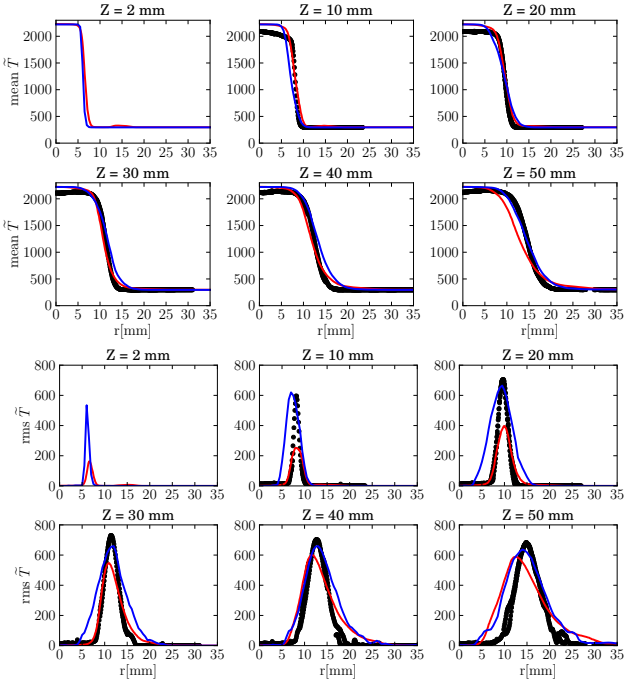

Figure 6. Mean (top) and RMS (bottom) temperature $\widetilde{T}$ profiles for the stratified (SwB5) case. Legend : — FSD model - P1 mesh. — F-TACLES model - Y1 mesh. • • Experiments.

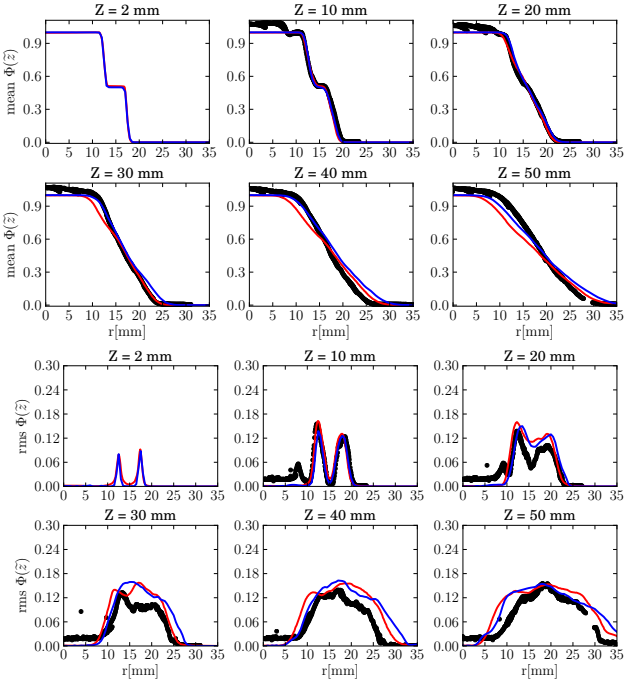

Figure 7. Mean (top) and RMS (bottom) equivalence ratio $\Phi(\widetilde{z})$ profiles for the stratified (SwB5) case. Legend : — FSD model - P1 mesh. — F-TACLES model - Y1 mesh. • • Experiments.

REFERENCES

Auzillon, P., Gicquel, O., Darabiha, N., Veynante, D. & Fiorina, B. 2012 A filtered tabulated chemistry model for les of stratified flames. *Combustion and Flame* **159** (8), 2704 – 2717.

Barlow, R. S., Dunn, M. J., Sweeney, M. S. & Hochgreb, S. 2012 Effects of preferential transport in turbulent bluff-body-stabilized lean premixed ch4/air flames. *Combustion and Flame* **159** (8), 2563 – 2575.

Boger, M., Veynante, D., Boughanem, H. & Trouvé, A. 1998 Direct numerical simulation analysis of flame surface density concept for large eddy simulation of turbulent premixed combustion. In *Proceedings of the Combustion Institute 27*, pp. 917 – 925. The Combustion Institute: Pittsburgh, Penn.

Bray, K., Domingo, P. & Vervisch, L. 2005 Role of the progress variable in models for partially premixed turbulent combustion. *Combustion and Flame* **141** (4), 431 – 437.

Charlette, F., Meneveau, C. & Veynante, D. 2002 A power-law flame wrinkling model for les of premixed turbulent combustion, part i: non-dynamic formulation. *Combustion and Flame* **131** (1/2), 159–180.

Domingo, P., Vervisch, L. & Bray, K. N. C. 2002 Partially premixed flamelets in les of nonpremixed turbulent combustion. *Combustion Theory and Modelling* **6** (4), 529–551.

Dunn, M. J. & Barlow, R. S. 2013 Effects of preferential transport and strain in bluff body stabilized lean and rich premixed ch4/air flames. *Proceedings of the Combustion Institute* **34** (1), 1411 – 1419.

Duwig, C. & Fureby, C. 2007 Large eddy simulation of unsteady lean stratified premixed combustion. *Combustion and Flame* **151** (1–2), 85 – 103.

Fiorina, B., Vicquelin, R., Auzillon, P., Darabiha, N., Gicquel, O. & Veynante, D. 2010 A filtered tabulated chemistry model for les of premixed combustion. *Combustion and Flame* **157** (3), 465 – 475.

Floyd, J., Kempf, A. M., Kronenburg, A. & Ram, R. H. 2009 A simple model for the filtered density function for passive scalar combustion les. *Combustion Theory and Modelling* **13** (4), 559–588.

Franchetti, B. M., Marincola, F. C., Navarro-Martinez, S. & Kempf, A. M. 2013 Large eddy simulation of a pulverised coal jet flame. *Proceedings of the Combustion Institute* **34** (2), 2419 – 2426.

Fureby, C. 2005 A fractal flame-wrinkling large eddy simulation model for premixed turbulent combustion. *Proceedings of the Combustion Institute* **30** (1), 593 – 601.

Gicquel, O., Darabiha, N. & Thévenin, D. 2000 Laminar premixed hydrogen / air counterflow flame simulations using flame prolongation of ildm with differential diffusion. *Proceedings of the Combustion Institute* **28** (2), 1901–1908.

Katta, V. & Roquemore, W. M. 2013 C/h atom ratio in recirculation-zone-supported premixed and nonpremixed flames. *Proceedings of the Combustion Institute* **34** (1), 1101 – 1108.

Kempf, A. M., Klein, M. & Janicka, J. 2005 Efficient generation of initial- and inflow-conditions for transient turbulent flows in arbitrary geometries. *Flow Turbulence and Combustion* **74** (1), 67–84.

Klein, M., Sadiki, A. & Janicka, J. 2003 A digital filter based generation of inflow data for spatially developing direct numerical or large eddy simulations. *Journal of Computational Physics* **186** (2), 652 – 665.

Lindstedt, P. 1997 12 month progree report 1. report no. tr-96 009. *Tech. Rep.*. Brite Euram Program Project BE 95 1523.

Ma, T., Stein, O., Chakraborty, N. & Kempf, A. M. 2013 A-

posteriori testing of algebraic flame surface density models for les. *Combustion Theory and Modelling* **accepted for publication**.

Marincola, F. C., Ma, T. & Kempf, A. M. 2013 Large eddy simulations of the darmstadt turbulent stratified flame series. *Proceedings of the Combustion Institute* **34** (1), 1307 – 1315.

Moureau, V., Domingo, P. & Vervisch, L. 2011 Design of a massively parallel cfd code for complex geometries. *Comptes Rendus Mécanique* **339** (2-3), 141 – 148.

Nambully, S. K. 2013 A filtered-laminar-flame pdf subgrid scale closure for les of premixed turbulent flames. application to a stratified bluff-body burner with differential diffusion. PhD thesis, INSA Rouen.

Nicoud, F., Toda, H. B., Cabrit, O., Bose, S. & Lee, J. 2011 Using singular values to build a subgrid-scale model for large eddy simulations. *Physics of Fluids* **23** (8), 085106.

Sweeney, M. S., Hochgreb, S., Dunn, M. J. & Barlow, R. S. 2011 A comparative analysis of flame surface density metrics inpremixed and stratified flames. *Proceedings of the Combustion Institute* **33** (1), 1419 – 1427.

Sweeney, M. S., Hochgreb, S., Dunn, M. J. & Barlow, R. S. 2012*a* The structure of turbulent stratified and premixed methane/air flames i: Non-swirling flows. *Combustion and Flame* **159** (9), 2896–2911.

Sweeney, M. S., Hochgreb, S., Dunn, M. J. & Barlow, R. S. 2012*b* The structure of turbulent stratified and premixed methane/air flames ii: Swirling flows. *Combustion and Flame* **159** (9), 2912 – 2929.

Sweeney, M. S., Hochgreb, S., Dunn, M. J. & Barlow, R. S. 2013 Multiply conditioned analyses of stratification in highly swirling methane/air flames. *Combustion and Flame* **160** (2), 322 – 334.

Veynante, D. & Vervisch, L. 2002 Turbulent combustion modeling. *Progress in Energy and Combustion Science* **28** (3), 193 – 266.

Wang, G., Boileau, M. & Veynante, D. 2011 Implementation of a dynamic thickened flame model for large eddy simulations of turbulent premixed combustion. *Combustion and Flame* **158** (11), 2199 – 2213.

Zhou, R., Balusamy, S., Sweeney, M. S., Barlow, R. S. & Hochgreb, S. 2013 Flow field measurements of a series of turbulent premixed and stratified methane/air flames. *Combustion and Flame* **in press**.